Vol 459|25 June 2009|doi:10.1038/nature08101

LETTERS

Enhanced carbon pump inferred from relaxation of nutrient limitation in the glacial ocean

L. E. Pichevin[1], B. C. Reynolds[2], R. S. Ganeshram[1], I. Cacho[3], L. Pena[3], K. Keefe[4] & R. M. Ellam[4]

The modern Eastern Equatorial Pacific (EEP) Ocean is a large oceanic source of carbon to the atmosphere[1]. Primary productivity over large areas of the EEP is limited by silicic acid and iron availability, and because of this constraint the organic carbon export to the deep ocean is unable to compensate for the outgassing of carbon dioxide that occurs through upwelling of deep waters. It has been suggested that the delivery of dust-borne iron to the glacial ocean[2,3] could have increased primary productivity and enhanced deep-sea carbon export in this region, lowering atmospheric carbon dioxide concentrations during glacial periods. Such a role for the EEP is supported by higher organic carbon burial rates documented in underlying glacial sediments[4,5], but lower opal accumulation rates cast doubts on the importance of the EEP as an oceanic region for significant glacial carbon dioxide drawdown[6,7]. Here we present a new silicon isotope record that suggests the paradoxical decline in opal accumulation rate in the glacial EEP results from a decrease in the silicon to carbon uptake ratio of diatoms under conditions of increased iron availability from enhanced dust input. Consequently, our study supports the idea of an invigorated biological pump in this region during the last glacial period that could have contributed to glacial carbon dioxide drawdown. Additionally, using evidence from silicon and nitrogen isotope changes, we infer that, in contrast to the modern situation, the biological productivity in this region is not constrained by the availability of iron, silicon and nitrogen during the glacial period. We hypothesize that an invigorated biological carbon dioxide pump constrained perhaps only by phosphorus limitation was a more common occurrence in low-latitude areas of the glacial ocean.

The EEP is an important area of biogenic opal production and burial in the ocean[8], accounting for two-thirds of the marine carbon dioxide efflux to the atmosphere today[1]. This is because primary productivity in the EEP is co-limited by silicic acid and iron availability[9] and so the biological carbon dioxide pump is unable to compensate for the upwelling of carbon dioxide[10] (Fig. 1).

In Fig. 2, we present glacial–interglacial records of biogenic accumulation as well as stable nitrogen and silicon isotope records spanning the past 35,000 years from an EEP marine sediment Ocean Drilling Program (ODP) Core 1240 (Fig. 1). Organic carbon concentrations in the sediment during the Last Glacial Maximum (LGM) were twice those of the Holocene and peaked during the deglacial period. The ^{230}Th-normalized organic carbon accumulation rates also show the same trend (Fig. 2). The doubling of organic carbon accumulation during the LGM is in agreement with previous studies showing that organic carbon export in the EEP was higher during the LGM[4,5] and may imply an invigorated biological carbon dioxide pump during this period (see Supplementary Information). Contradicting such an assertion, opal concentration in Core 1240 was reduced roughly by a factor of two during the LGM, consistent with existing opal accumulation records in the region[6,7]. Such differences in biogenic accumulation records cannot be explained by local changes in upwelling alone.

The sedimentary ratio of silicon to organic carbon (Si:C) in Core 1240 increases drastically during the glacial to interglacial transition with values during the early Holocene almost three times higher than during the LGM (Fig. 2). This change in the relative accumulation of opal and carbon is seen across the entire EEP and therefore cannot be explained simply by factors such as differential distribution and preservation of these biogenic components (Supplementary Information).

The contrast between opal and organic carbon accumulation trends during the LGM in the EEP could be reconciled by invoking a shift in the phytoplankton communities from diatomaceous to coccolithophorid production. This would have reduced the carbon rain-rate ratios (the relative contributions of organic carbon and carbonate to total export production) in the glacial EEP and hence the capacity of the marine carbon reservoir to sequester carbon[11]. However, carbonate contents and accumulation rates in Core 1240 do not show a clear glacial–interglacial pattern to support such a shift

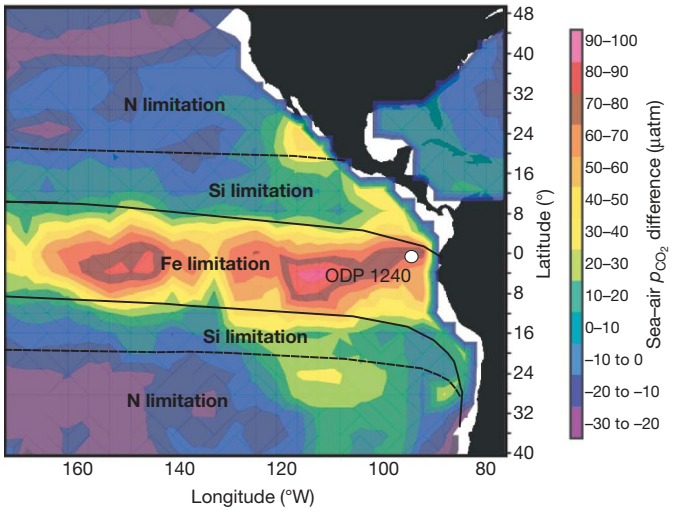

Figure 1 | Annually averaged carbon dioxide partial pressure (p_{CO_2}) difference between the atmosphere and the ocean for 1995. Data modified from ref. 1; see http://www.ldeo.columbia.edu/res/pi/CO2/. Also depicted is the hierarchy of nutrient limitation for diatom growth across the low-latitude Pacific Ocean. Black lines delimit the area where the most severe limitation is imposed by iron, dotted lines delimit the area of silicic acid limitation. Beyond these lines the ocean is first nitrate-limiting (modified from ref. 9). We note the geographical correspondence between carbon dioxide efflux maxima (warm colours) and iron and silicic acid limitation areas. The site of ODP 202 Core 1240 is shown with a white dot.

[1]School of Geosciences, Grant Institute, University of Edinburgh, West Main Road, EH10 3JW, Edinburgh, UK. [2]IGMR, ETH Zürich, Clausiusstrasse 25, CH-8092 Zürich, Switzerland. [3]GRC Geociències Marines, Facultat de Geologia, Universitat de Barcelona C/ Martí Franques s/n 08028 Barcelona, Spain. [4]Scottish Universities Environment Research Centre, Rankine Avenue, Scottish Enterprise Technology Park, East Kilbride, G75 0QF, UK.

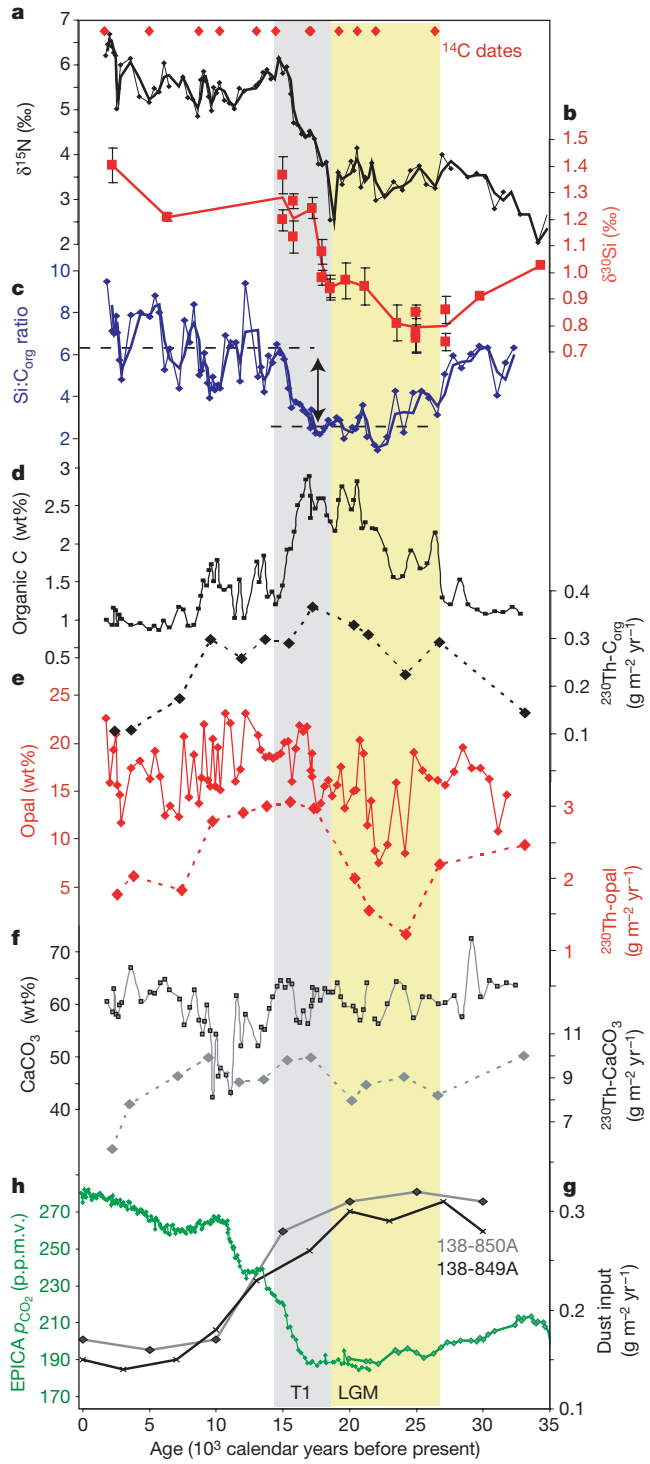

Figure 2 | Sedimentary records from Core 1240 plotted versus calendar ages before present. **a**, $\delta^{15}N$ signal of bulk material (the bold line indicates the 2-point average). **b**, The $\delta^{30}Si$ signal of diatoms (error bars are 1 sigma error of the mean). **c**, Si:C ratio (the bold line indicates the 2-point average). **d**–**f**, Elemental concentrations (solid lines) and ^{230}Th-normalized accumulation rates (dotted lines) of organic carbon (**d**), opal (**e**) and carbonate (**f**). **g**, Dust fluxes in Core ODP 138-849A and 138-850A (ref. 2). **h**, Atmospheric p_{CO_2} record from the EPICA (European Project for Ice Coring in Antarctica) dome C ice core[31] in p.p.m.v., parts per million by volume. T1, Termination 1.

in the rain-rate ratio of particulate export (Fig. 2). The estimates of carbonate accumulation rates in the EEP based either on the ^{230}Th-normalization technique or on high-resolution ^{14}C stratigraphy unequivocally document reduced carbonate fluxes and production during the LGM[12]. Moreover, a recent study[13] of carbonate accumulation corrected for sedimentary dissolution has even suggested that primary production in the EEP shifted from carbonate to opal production during the LGM compared to the Holocene. Therefore, the sedimentary opal records from the EEP showing halved accumulation rates during the LGM compared to the Holocene epoch[7], thus implying a less efficient biological carbon dioxide pump, contradict the inferences based on enhanced organic carbon production and have puzzled researchers. Resolving this paradox has important implications in understanding the role of the EEP in glacial carbon dioxide drawdown and the impact of enhanced iron delivery on nutrient limitation and the biological carbon dioxide pump during the glacial periods.

Availability of silicic acid in the surface water of the EEP is considered the major control on opal production[10]—a view that stems from modern observations of silicon limitation in this region (Fig. 1). However, LGM conditions could have been drastically different for diatom growth when dust-borne iron delivery to the surface EEP was twice as much as it is today, as recorded by sediment cores in this area[2,3] (Fig. 2). The impact of this increased iron delivery on opal production in the iron-limited low-latitude Pacific Ocean[2,3] has never been fully explored. Results from *in situ* iron-fertilization experiments[14,15] reveal that the alleviation of iron limitation in the EEP causes a two- to threefold decrease in Si:C uptake ratios of siliceous producers, owing to decreased cell silicification[14,15]. If this were to happen during the iron-replete LGM, lower silicon uptake during diatom growth may have resulted and consequently reduced opal accumulation. In addition, given the large decline in Si:C uptake ratios documented in these experiments, surplus silicic acid may have been available during diatom production. Thus, the reconstruction of glacial silicic acid utilization in the EEP could allow us to unravel the opal accumulation paradox and to resolve the carbon mass balance during the LGM.

We evaluate the possibility of lowered silicon utilization during diatom growth under iron-replete glacial periods using a record of $\delta^{30}Si$ in opal (Fig. 2). During the Holocene $\delta^{30}Si$ values are about +1.3‰, a value close to the isotopic composition of silicic acid in intermediate water masses of the tropical Pacific[16,17]. This indicates near-complete utilization of the available silicic acid, consistent with modern observations of its limitation in the EEP (Supplementary Information). In contrast, the LGM values were much lower (<0.9‰). This lower $\delta^{30}Si$ signature may reflect a decrease in the relative utilization of silicic acid in the EEP during the glacial period, provided this shift is not affected by glacial change in the nutrient source.

During the glacial period, silicic acid leakage from the Southern Ocean, whereby enhanced dust-borne iron input to the Southern Ocean resulted in the conservation of silicic acid over other nutrients, leading to its export to low latitudes[18,19], is one mechanism that could have potentially altered silicic acid supply to the EEP and its isotopic signature. It has been estimated that during the glacial period, the low-latitude Pacific could have received three times more silicic acid through the subantarctic mode waters, with $\delta^{30}Si$ values ranging from 1.7‰ to 3‰[17,20]. The resulting change in source signature can at best account only for a very modest decline in the glacial diatom-bound silicon isotope signal (~0.1‰, assuming the minimum value of 1.7‰ for the Southern Ocean source). However, given the range of values for the subantarctic source, heavier shifts in glacial sediments are more probable (see Supplementary Information). Additionally, the threefold increase in the supply of $Si(OH)_4$ to the EEP should have increased glacial opal burial. On the contrary, Core 1240 records a glacial decline in opal accumulation with markedly lighter isotopic values (Fig. 2).

The reason for the apparent contrast becomes clear if we consider how the glacial increase in dust-borne iron inputs would have affected silicic acid utilization locally within the EEP. The increased iron input and the resultant decline in Si:C uptake ratios, as proposed for the

Southern Ocean, should also have operated in the glacial EEP, leading to the conservation of silicic acid[14,18]. This would explain the decline in opal accumulation and the lighter δ^{30}Si values in the glacial intervals of Core 1240. Paradoxically, the increased silicic acid supply from the Southern Ocean appears to have occurred at the time the demand for this nutrient declined locally within the EEP—a contention that is supported by the similar glacial–interglacial histories of dust input in these two regions[3]. Although regional patterns in glacial silicic acid utilization need further examination, this new result documenting excess silicic acid in the glacial EEP strongly implies that the decline in opal accumulation in LGM sediments is not controlled by the availability of silicic acid but is most probably the consequence of iron fertilization and lowered Si:C uptake ratios during diatom growth. Importantly, the glacial decrease in opal accumulation observed across the EEP[6,7] does not reflect a decline in carbon rain-rate ratio and the biological carbon dioxide pump, as was previously suggested[6].

Our results suggest that the glacial scenario of nutrient limitation and the constraints on biological production in the EEP were drastically different from the modern situation depicted in Fig. 1. In contrast to modern conditions, enhanced iron delivery and the resultant switch to lower Si:C uptake ratio by diatoms led to conditions where iron and silicon are no longer limiting factors for biological productivity. From glacial δ^{30}Si values in Core 1240, and applying a steady-state model[17] we estimate that relative silicic acid utilization during the LGM declined by about 25% from a near-complete utilization during the Holocene. This calculation assumes a constant $Si(OH)_4$ source of around +1.2‰, in agreement with low-latitude Pacific intermediate-water values[16,17]. This estimate of decreased $Si(OH)_4$ utilization would be even greater if the leakage of isotopically heavy silicic acid from subantarctic waters is taken into account[20]. Similarly, the nitrogen-isotope record allows us to assess the potential for glacial nitrate limitation. The absence of iron and silicon co-limitation during the glacial period should have led to increased nitrate utilization and heavier glacial δ^{15}N.

In contrast, the N-isotope profile (Fig. 2) shows a trend towards lower δ^{15}N values during the LGM relative to the Holocene, consistent with other, similar studies in this region[21]. However, given that nitrate utilization is incomplete in the modern EEP, a further δ^{15}N decrease (>3‰) during the glacial period cannot be explained simply by changes in nitrate uptake by biota alone because this would entail a very large reduction in nitrate utilization. Therefore, we suggest that the low LGM δ^{15}N values relative to the Holocene reflect an additional supply of isotopically lighter nitrogen due to reduced denitrification in the oxygen minimum zones off Peru and Mexico[22,23]. Today, the prevalence of denitrification in these margins bordering the EEP means that the source waters supplied to the EEP thermocline are depleted in nitrate relative to phosphate (lower than the Redfield N:P value) and have a relatively heavy nitrogen-isotope signature (+6.5‰ as opposed to the +4.8‰ ocean average) owing to mixing with partially denitrified heavy nitrate[24]. Thus, reduced denitrification during glacial periods would enhance the nitrate inputs into the EEP by increasing the N:P ratio of upwelling waters and provide nitrate that is isotopically lighter. In combination, both these factors would lead to a shift to lighter sedimentary nitrogen-isotope signatures irrespective of any glacial change in local upwelling[25,26]. Thus, the lighter N-isotope values provide evidence that nitrate is also not a limiting nutrient in the glacial EEP—a condition comparable to the modern situation. Therefore, the data strongly suggest simultaneous removal of the constraints imposed by iron, silicon and nitrogen limitation on biological production in the EEP during the LGM.

This argues for a more invigorated biological carbon dioxide pump in the glacial EEP, perhaps ultimately constrained by the availability of dissolved phosphate. The resulting increase in carbon export and rain-rate ratio as documented in the glacial sediments of the EEP (Supplementary Information) should have reduced carbon dioxide evasion. Such an assertion is also consistent with the timing of the first phase of the atmospheric carbon dioxide rise during the last glacial termination (~18,000 years ago) which is contemporaneous (within dating uncertainties) with the decline in dust delivery and the increases in sedimentary Si:C and δ^{30}Si in EEP records.

Finally, we suggest that our results have much wider ramifications: the EEP provides an illustration of the constraints imposed on the biological carbon dioxide pump in low-latitude oceans of the glacial periods. In currently iron-limited open-ocean 'high-nitrate, low-chlorophyll' regions, such as the EEP and the Southern Ocean, the switch to iron-replete LGM conditions has led to the generation of excess silicic acid during diatom growth, which in turn is subject to dispersal through surface and subsurface ocean circulation, increasing the availability of silicic acid over a much wider area of the glacial ocean[18,19]. This additional silicic acid supply occurs at a time when its demand by biota is already reduced by iron fertilization, which should have caused drastic reductions in silicon limitation over large areas of the glacial ocean.

Also, the documented glacial decline in denitrification in the world's oxygen minimum zones is expected to have increased the availability of nitrate[23,27]. For instance, the NO_3:PO_4 ratio at the surface of the modern EEP is about 12.5 (that is, lower than the Redfield N:P ratio of 16). In contrast, a 30% increase in nitrate inventory during the last glacial period compared to today, as suggested by modelling work[28], could have been sufficient to cause the N:P ratio in the EEP to exceed the Redfield ratio. Such changes, occurring more widely, would have resulted in an invigorated carbon dioxide pump in low-latitude oceans ultimately constrained by the availability of dissolved phosphate, as suggested by the case study reported here and predicted by recent model results[29]. Therefore, we hypothesize that phosphorus limitation was much more widespread during the glacial periods—a situation fundamentally different to that of the modern ocean.

METHODS SUMMARY

ODP 202 Core 1240 was retrieved from the Cocos ridge (00°01.31′ N; 86°27.76′ W; 2,921 m depth) in the EEP. The age model is based on 13 accelerator mass spectrometry (AMS) ^{14}C dates on planktonic foraminifers[25]. Determination of the opal content (wt%) was performed by molybdate-blue spectrophotometry on alkaline extracts. Organic carbon (wt%), total nitrogen (wt%) and δ^{15}N (wt‰) were determined on 10 mg of freeze-dried and powdered bulk sediments using a Carlo Erba elemental analyser coupled to a VG Prism III mass spectrometer at the University of Edinburgh. ^{230}Th normalization was performed using acid digestion on bulk samples and column chemistry followed by multiple-collector inductively coupled plasma mass spectrometry (MC-ICPMS) analyses. Purification of the diatom samples for silicon isotope measurement was performed by chemical leaching of the carbonate and organic fractions, sieving and differential settling. Silicon isotope determination was conducted in ETH Zürich on the Nu1700 high-resolution MC-ICPMS[30].

Full Methods and any associated references are available in the online version of the paper at www.nature.com/nature.

Received 1 April 2008; accepted 23 April 2009.

1. Takahashi, T. *et al.* Global sea-air CO_2 flux based on climatological surface ocean pCO_2, and seasonal biological and temperature effects. *Deep-Sea Res. II* **49**, 1601–1622 (2002).
2. McGee, D., Marcantonio, F. & Lynch-Stieglitz, J. Deglacial changes in dust flux in the eastern equatorial Pacific. *Earth Planet. Sci. Lett.* **257**, 215–230 (2007).
3. Winckler, G., Anderson, R. F., Fleisher, M. Q., McGee, D. & Mahowald, N. Covariant glacial-interglacial dust fluxes in the equatorial Pacific and Antarctica. *Science* **320**, 93–96 (2008).
4. Pedersen, T. F. Increased productivity in the eastern equatorial Pacific during the Last Glacial Maximum (19,000 to 14,000 yr BP). *Geology* **11**, 16–19 (1983).
5. Lyle, M. Climatically forced organic-carbon burial in equatorial Atlantic and Pacific oceans. *Nature* **335**, 529–532 (1988).
6. Kienast, S. S., Kienast, M., Jaccard, S., Calvert, S. E. & Francois, R. Testing the silica leakage hypothesis with sedimentary opal records from the eastern equatorial Pacific over the last 150 kyrs. *Geophys. Res. Lett.* **33**, doi:10.1029/2006GL026651 (2006).
7. Bradtmiller, L. I., Anderson, R. F., Fleisher, M. Q. & Burckle, L. H. Diatom productivity in the equatorial Pacific Ocean from the last glacial period to the present: A test of the silicic acid leakage hypothesis. *Paleoceanography* **21**, doi:10.1029/2006PA001282 (2006).
8. Lisitzin, A. P. in *The Micropalaeontology of Oceans Symposium, Illustrated Maps* 173–195 (Cambridge University Press, 1971).

9. Moore, J. K., Doney, S. C. & Lindsay, K. Upper ocean ecosystem dynamics and iron cycling in a global three-dimensional model. *Glob. Biogeochem. Cycles* **18,** doi:10.1029/2004GB002220 (2004).
10. Dugdale, R. C. & Wilkerson, F. P. Silicate regulation of new production in the equatorial Pacific upwelling. *Nature* **391,** 270–273 (1998).
11. Archer, D. & Maier-Reimer, E. Effect of deep-sea sedimentary calcite preservation on atmospheric CO_2 concentration. *Nature* **367,** 260–263 (1994).
12. Loubere, P. & Richaud, M. Some reconciliation of glacial-interglacial calcite flux reconstructions for the eastern equatorial Pacific. *Geochem. Geophys. Geosyst.* **8,** doi:10.1029/2006GC001367 (2007).
13. Richaud, M., Loubere, P., Pichat, S. & Francois, R. Changes in opal flux and the rain ratio during the last 50,000 years in the equatorial Pacific. *Deep-Sea Res. II* **54,** 762–771 (2007).
14. Takeda, S. Influence of iron availability on nutrient consumption ratio of diatoms in oceanic waters. *Nature* **393,** 774–777 (1998).
15. Hutchins, D. A. & Bruland, K. W. Iron-limited diatom growth and Si: N uptake ratios in a coastal upwelling regime. *Nature* **393,** 561–564 (1998).
16. Reynolds, B. C., Frank, M. & Halliday, A. N. Silicon isotope fractionation during nutrient utilization in the North Pacific. *Earth Planet. Sci. Lett.* **244,** 431–443 (2006).
17. Beucher, C. P., Brzezinski, M. A. & Jones, J. L. Sources and biological fractionation of silicon isotopes in the eastern equatorial Pacific. *Geochim. Cosmochim. Acta* **72,** 3063–3073 (2008).
18. Brzezinski, M. A. *et al.* A switch from $Si(OH)_4$ to NO_3 depletion in the glacial Southern Ocean. *Geophys. Res. Lett.* **29,** doi:10.1029/2001GL014349 (2002).
19. Matsumoto, K., Sarmiento, J. L. & Brzezinski, M. A. Silicic acid leakage from the Southern Ocean: A possible explanation for glacial atmospheric pCO_2. *Glob. Biogeochem. Cycles* **16,** doi:10.1029/2001GB001442 (2002).
20. Beucher, C. P., Brzezinski, M. A. & Crosta, X. Silicic acid dynamics in the glacial sub-Antarctic: implications for the silicic acid leakage hypothesis. *Glob. Biogeochem. Cycles* **21,** doi:10.1029/2006GB002746 (2007).
21. Farrell, J. W., Pedersen, T. F., Calvert, S. E. & Nielsen, B. Glacial–interglacial changes in nutrient utilization in the equatorial Pacific Ocean. *Nature* **377,** 514–517 (1995).
22. Toggweiler, J. R. & Carson, S. in *Upwelling in the Ocean: Modern Processes and Ancient Records* (eds Summerhayes, C. P., Emeis, K.-C., Angel, M. V., Smith, R. L. & Zeitzschel, B.) 337–360 (John Wiley & Sons, 1995).
23. Ganeshram, R. S., Pedersen, T. F., Calvert, S. E., McNeill, G. W. & Fontugne, M. R. Glacial-interglacial variability in denitrification in the world's oceans: causes and consequences. *Paleoceanography* **15,** 361–376 (2000).
24. Altabet, M. A. Nitrogen isotopic evidence for micronutrient control of fractional NO3- utilization in the equatorial Pacific. *Limnol. Oceanogr.* **46,** 368–380 (2001).
25. Pena, L. D., Cacho, I., Ferretti, P. & Hall, M. A. El Niño–Southern Oscillation–like variability during glacial terminations and interlatitudinal teleconnections. *Paleoceanography* **23,** doi:10.1029/2008PA001620 (2008).
26. Koutavas, A., Lynch-Stieglitz, J., Marchitto, T. M. & Sachs, J. P. El Nino-like pattern in ice age tropical Pacific sea surface temperature. *Science* **297,** 226–230 (2002).
27. Ganeshram, R. S., Pedersen, T. F., Calvert, S. E. & Francois, R. Reduced nitrogen fixation in the glacial ocean inferred from changes in marine nitrogen and phosphorus inventories. *Nature* **415,** 156–159 (2002).
28. Deutsch, C., Sigman, D. M., Thunell, R. C., Meckler, A. N. & Haug, G. H. Isotopic constraints on glacial/interglacial changes in the oceanic nitrogen budget. *Glob. Biogeochem. Cycles* **18,** doi:10.1029/2003GB002189 (2004).
29. Moore, J. K. & Doney, S. C. Iron availability limits the ocean nitrogen inventory stabilizing feedbacks between marine denitrification and nitrogen fixation. *Glob. Biogeochem. Cycles* **21,** doi:10.1029/2006GB002762 (2007).
30. Georg, R. B., Reynolds, B. C., Frank, M. & Halliday, A. N. New sample preparation techniques for the determination of Si isotopic compositions using MC-ICPMS. *Chem. Geol.* **235,** 95–104 (2006).
31. Monnin, E. *et al.* Atmospheric CO_2 concentrations over the last glacial termination. *Science* **291,** 112–114 (2001).

Supplementary Information is linked to the online version of the paper at www.nature.com/nature.

Acknowledgements We thank R. Francois, S. Kienast, W. Geibert, E. Galbraith and G. Leduc for discussions. Funding for this project was provided by the Scottish Alliance for Geoscience Environment Society (SAGES), the Natural Environment Research Council (NERC) through a Standard NERC grant (to R.S.G. and L.E.P.) and a Marie Curie Intra-European fellowship (to L.E.P.). I.C. and L.P. acknowledge funding from the ROMIAT and GRACCIE-CONSOLIDER projects.

Author Contributions L.E.P. and R.S.G. initiated the project. L.E.P. and B.C.R. measured silicon isotopes in ETH Zurich, L.E.P. measured elemental composition and nitrogen isotopes, L.E.P., K.K. and R.M.E. made the ^{230}Th measurements. I.C. and L.P. provided the age model. L.E.P. and R.S.G. wrote the paper with the participation of B.R.C. All authors participated in the discussions on the results and commented on the manuscript.

Author Information Reprints and permissions information is available at www.nature.com/reprints. Correspondence and requests for materials should be addressed to L.E.P. (laetitia.pichevin@ed.ac.uk).

METHODS

ODP 202 Core 1240 was retrieved from the Cocos ridge (see ODP report http://www-odp.tamu.edu/publications/202_IR/chap_11/chap_11.htm).

Determination of the opal content (wt%) was performed according to the method published in ref. 32. ^{230}Th normalization was used to account for the effect of sediment focusing[33] and performed at the Scottish Universities Environment Research Centre[34] (Supplementary Information).

Purification of the diatom samples for silicon isotope measurement was performed following a cleaning method published recently[35]. A small amount of biogenic opal (0.5 mg) was dried down with concentrated perchloric acid at ~180 °C in Teflon vials, and then dissolved in 100 µl of 1 M NaOH, before being diluted to 5 ml with 0.01 M HCl after 24 h. An equivalent to 10 µg of opal was loaded onto a pre-cleaned 1.8 ml DOWEX 50W-X12 cation exchange resin bed (in H^+ form) and eluted with 5 ml of purified water (Milli-Q element 18.2 MΩ cm^{-1}). The silicon isotope composition was determined on the diluted solution (0.6 p.p.m. Si) on the Nu1700 high-resolution MC-ICPMS at ETH Zürich, using a standard-sample-standard bracketing protocol. All results in this study were calculated using the δ^{30}Si notation for deviations of the measured ^{30}Si/^{28}Si from the international silicon standard NBS28 in parts per thousand (‰). The long-term reproducibility was better than 0.07‰ δ^{30}Si (one standard deviation, s.d.)[36]. Samples were measured at least five times, which resulted in a 95% confidence level below 0.08‰. Error bars on the δ^{30}Si plot are calculated as 1 sigma error of the mean (Fig. 2).

32. Mortlock, R. A. & Froelich, P. N. A simple method for the rapid determination of biogenic opal in pelagic marine sediments. *Deep-Sea Res. A* **36,** 1415–1426 (1989).
33. Francois, R., Frank, M., van der Loeff, M. M. R. & Bacon, M. P. Th-230 normalization: an essential tool for interpreting sedimentary fluxes during the late Quaternary. *Paleoceanography* **19,** doi:10.1029/2003PA000939 (2004).
34. Ellam, R. M. & Keefe, K. MC-ICP-MS analysis of non-natural U isotope ratios using a Th-229/Th-232 external mass bias correction. *J. Anal. At. Spectrom.* **22,** 147–152 (2007).
35. Morley, D. W. *et al.* Cleaning of lake sediment samples for diatom oxygen isotope analysis. *J. Paleolimnol.* **31,** 391–401 (2004).
36. Reynolds, B. C., Georg, R. B., Oberli, F., Wiechert, U. H. & Halliday, A. N. Re-assessment of silicon isotope reference materials using high-resolution multi-collector ICP-MS. *J. Anal. At. Spectrom.* **21,** 266–269 (2006).